

Fragment size- and dose-specific effects of hyaluronan on matrix synthesis by vascular smooth muscle cells

Binata Joddar^a, Anand Ramamurthi^{a,b,*}

^aDepartment of Bioengineering, Clemson University, Clemson, SC, USA

^bDepartment of Cell Biology and Anatomy, Medical University of South Carolina, Charleston, SC 29425, USA

Received 26 August 2005; accepted 13 January 2006

Abstract

Tissue engineering of vascular elastin matrices disrupted by mechanical injury, disease, or congenitally absent, is among other factors, limited by the lack of suitable cell scaffolds to up-regulate and guide innately poor elastin synthesis by adult vascular smooth muscle cells (SMCs). Evidence suggests that scaffolds based on hyaluronan (HA), a glycosaminoglycan, may be useful to elicit elastogenic cell responses, although these effects appear to be dictated by HA fragment size and/or dose. This study investigates the efficacy of a simple, frequently adopted exogenous HA supplementation model to test this hypothesis. Rat aortic SMCs were cultured with HA (2×10^6 Da (HMW) \geq MW $\leq 2.2 \times 10^4$ Da) supplemented at doses between 0.2 and 200 μ g/ml. Cell layers were biochemically assayed for DNA, elastin and collagen content. Fragmented, but not high molecular weight (HMW) HA, stimulated cell proliferation in inverse correlation fragment size while the opposite effect was observed for synthesis of soluble and matrix elastin; almost no dose effects were observed within any group. SDS-Page/Western Blot and a desmosine assay semi-quantitatively confirmed the observed biochemical trends for tropoelastin and matrix elastin, respectively. Quantitative differences in elastin deposition were mirrored in TEM micrographs. Elastin was mostly deposited in the form of amorphous clumps but fibers were increasingly present in cell layers cultured with HMW HA. HA and its fragments did not disrupt normal fibrillin-mediated mechanisms of elastin matrix deposition. While the current outcomes confirm that the effects of HA on elastin synthesis are fragment size-specific, this study shows that an exogenous supplementation model does not necessarily simulate cellular matrix synthesis responses to HA-based biomaterial scaffolds.

© 2006 Elsevier Ltd. All rights reserved.

Keywords: Elastin; Regeneration; Vascular; Extracellular matrix; Glycosaminoglycan; Hyaluronan

1. Introduction

Elastin is a critical structural protein distributed in the extracellular matrix of connective tissues (e.g., blood vessels, oesophagus, skin) that need to stretch and retract following mechanical loading and release [1]. In vascular tissues, smooth muscle cells (SMCs) synthesize elastin as a soluble monomer (tropoelastin), which is then post-translationally stabilized by cross-linking into an insoluble, structural matrix that forms 30–50% of dry tissue weight [2]. Vascular elastin is organized into bundles (lamellae)

that provide the necessary compliance to absorb and transmit hemodynamic forces [3], and permit vessel retraction to original dimensions after load release. At the cellular level, elastin also mechano-transduces SMC behavior [4] through binding to cell surface elastin–laminin receptors [5], and critically regulates vascular SMC activity during morphogenesis [6] and disease [7]. Thus, degradation of vascular elastin due to mechanical injury [8], as an etiological outcome of non-inherited diseases like atherosclerosis, or proliferative conditions such as aneurysms [9], or its congenital absence or deformation, can severely compromise vascular homeostasis. The replacement or preservation of elastin matrices is thus a high priority.

Previous attempts at preserving or regenerating elastin structures have focused on delivery of MMP inhibitors, and elastogenesis within synthetic [10] or tissue-engineered

*Corresponding author. Department of Bioengineering, Clemson University, Clemson, SC, USA. Tel.: +1 843 792 5853; fax: +1 843 792 0664.

E-mail address: aramamu@clemson.edu (A. Ramamurthi).

grafts [11] deployed in situ at the vascular injury/disease site. However, elastin synthesis is severely deficient within vascular grafts [12], likely due to progressive destabilization of tropoelastin mRNA expression in adult cells [13]. As an alternative, synthetic elastomers (e.g. polyhydroxyalkanoates, polyglycolic acid) [14,15], or elastin matrices isolated from xenogeneic (e.g., porcine) [16] or allogeneic (e.g., cadaveric, umbilical) [17] blood vessels have been used. While synthetic elastomers reinstate mechanical but not elastin-derived cell signaling mechanisms, elastin allografts and xenografts are limited, respectively by short supply of cadaveric tissues and the insufficiency of current chemical processing methods to completely extract immune-reactive donor-cells and contaminating epitopes/globular proteins, essential to prevent immune rejection [18] and calcification [19] in the host. Assembly of elastomers from polypeptide precursors [20,21] and fabrication of synthetic scaffolds designed to provide elastogenic cues are other popular strategies [22]. In this regard however, the use of natural ECM-based scaffolds is preferable due to their greater likelihood of evoking native integrin-ECM interactions and preserving native cell phenotype [23]. Accordingly, successful up-regulation of elastin synthesis and its organization into mature elastic tissue is crucially contingent on the selection of an appropriate scaffold material from among a sub-set of ECM molecules shown to actively facilitate elastogenesis in vivo.

Glycosaminoglycans (GAGs), a component of the ECM may be appropriate in this regard. In particular, hyaluronan (HA), a GAG has been implicated to play an indirect role in elastogenesis through its intimate binding of versican [24], which in turn interacts with microfibrillar proteins (fibulin-1, 2) and elastin-associated proteins to form higher-order macromolecular structures important elastic fiber assembly [25]. Other studies suggest that GAGs coacervate soluble tropoelastin molecules on their highly anionic surfaces, facilitating their lysyl oxidase (LOX)-mediated cross-linking into an insoluble matrix [26]. HA and other GAGs are also known to elastin fibers against elastase degradation [27]. These findings encourage the utility of HA biomaterials as elastogenic scaffolds. Suggestably, fragmented HA induces elastogenic responses, although native long-chain HA likely also plays a role in facilitating matrix deposition [28,29]. Although the biologic effects of HA are somewhat specific to cell type, these observations generally agree with previous reports that HA fragments, particularly oligos, interact more with cells [30]. Since HA fragments elicit inflammatory cell responses [31], HA scaffold design must necessarily follow an investigation into the fragment size and dose specific effects of HA on desired (e.g., elastogenic) and undesired (e.g., inflammatory) cell responses. To broadly assess the former aspect, here, we adopt a simple exogenous HA supplementation model to assess HA size and dose-specific differences in cellular responses with regard to matrix synthesis.

2. Materials and methods

The impact of exogenous bolus of HA of defined fragment sizes and doses on matrix synthesis by adult rat aortic SMCs (RASMCs) was studied over a period of 21 days. Control cell layers were cultured in absence of HA.

2.1. Preparation of HA bolus

Solutions of HA were prepared at stock concentrations of 1000, 100, 10 and 1 $\mu\text{g}/5\text{ ml}$ (effective concentrations of 200, 20, 2 and 0.2 $\mu\text{g}/\text{ml}$) and diluted 1:5 v/v in serum-rich DMEM:F12 medium (Invitrogen, Grand Island, NY). HA, procured as sodium hyaluronate salt (NaHA) containing average fragment sizes of $2 \times 10^6\text{ Da}$ (Genzyme Biosurgery, Cambridge, MA), $2 \times 10^5\text{ Da}$ (Genzyme), and $2 \times 10^4\text{ Da}$ (Lifecore Technologies, Chaska, MN), designated as high molecular weight (HMW), low molecular weight (LMW), and very low molecular weight (VLMW) HA, respectively, was dissolved in sterile serum-free culture medium (48 h, 4 °C), and filter-sterilized prior to addition to cell cultures.

2.2. Cell culture

Low passage (6–8) adult rat SMCs (Cell Applications, San Diego, CA) were selected for study due to their relatively lower levels of tropoelastin production compared to neonatal cells, thus of greater relevance to targeted regeneration of elastin in adult blood vessels. Stock cells were trypsinized (0.25% trypsin/0.1% (v/v) EDTA; Invitrogen), pelleted by centrifugation (500g, 7 min), resuspended in DMEM: F12 containing 10% (v/v) FBS and 1% (v/v) penicillin–streptomycin and seeded onto wells in a 6-well vacuum-plasma-treated polystyrene tissue culture plate (Becton Dickinson Labware, Franklin Lakes, NJ; Culture area = 10 cm^2) at a count of $10^5\text{ cells}/10\text{ cm}^2$. After overnight incubation, cells were cultured in the respective HA stock solution diluted in (1:5 v/v) serum-rich medium. Control cultures received HA-free DMEM: F12. All experimental trials and controls were performed in triplicate. Spent medium containing dissolved HA, was replaced twice weekly during the duration of culture, pooled and analyzed at the end of the 21 day culture period. Cells were also cultured in 4-well sterile chamber slides (Nalgene Nunc International, Rochester, NY) at a count of $10^4\text{ cells}/2.4\text{ cm}^2$. At 21 days, these cell layers were immunolabeled for detection of elastin and collagen in the matrix.

2.3. DNA assay for cell proliferation

The DNA content of the cell layers was used to assess the proliferation of SMCs in culture. The measured amounts of synthesized matrix were also normalized to the DNA content to provide a reliable basis of comparison between samples, and to broadly assess if the observed increases (if any) in the amount of matrix synthesized could possibly be due to increased levels of transcription. Broadly, cell layers at 1 and 21 days of culture were trypsinized, pelleted, resuspended in 1 ml of NaCl/Pi buffer (4M NaCl, 50mM Na_2HPO_4 , 2mM EDTA, 0.02% (w/v) Na Azide, and pH 7.4), and a 100- μl aliquot assayed. The DNA in the sonicated aliquot was measured using the fluorometric method described by Labarca and Paigen [32]. Actual cell counts were then calculated on the basis of 6pg DNA/cell, assuming this amount remained unchanged through the period of culture.

2.4. Biochemical analysis of the extracellular matrix

2.4.1. Hydroxy-proline (OH-Pro) assay for collagen

The collagen content of cell layers was estimated from their measured OH-Pro content as described previously [33]. For the OH-Pro assay, frozen 4ml aliquots containing the homogenized 3-week-old cell layers were thawed, centrifuged at 500g to isolate cell pellets (P1), which were then dried to a constant weight and digested with 1 ml of 0.1 N NaOH (1 h, 98 °C). The digestate was then centrifuged (2000g, 15 min) to isolate a

mass of insoluble, crosslinked elastin (P2). The supernatant (S1) containing solubilized collagen and immature matrix elastin was neutralized with an equal volume of 12N HCl, and divided into two equal volumetric halves. One half-volume was hydrolyzed at 110 °C for 16 h, and dried in a constant stream of N₂ gas over 3 h. Aliquots (20 µl) of the reconstituted residue were assayed. The measured amounts of OH-Pro were corrected to account for the 4% (w/w) of OH-Pro contained in solubilized elastin present in the reconstituted sample (S2; see Section 2.4.2). Finally, total amount of matrix-derived collagen was calculated on the basis of the 13.2% OH-Pro content of collagen [33].

2.4.2. *Fastin assay for elastin*

The fastin assay was used to quantify the total amount of elastin matrix within cell layers, and that released into the culture medium in a soluble form (tropoelastin). Elastin derived from the 21 day-old cell layers was assumed to be one of two types, namely, insufficiently cross-linked type digestible in alkali, and contained in fraction (S1), or of the mature, mostly highly cross-linked type contained in the insoluble pelleted fraction (P2). Since the fastin assay (Accurate Scientific and Chemical Corporation, Westbury, NY), quantifies only soluble α -elastin, the insoluble elastin was first reduced to a soluble form before subjecting to the assay. To do this, the elastin pellet (P2) was dried to a constant weight, solubilized with three cycles of treatment with 0.25N oxalic acid (1 h/cycle, 95 °C), and the pooled digests then filtered in microcentrifuge tubes fitted with LMW cut-off membranes (10,000 Da). The insufficiently cross-linked, soluble elastin fraction retained in the oxalic acid-free fraction (S3) and in the water-reconstituted hydrolysate (S2) were also quantified using the fastin assay. Spent fractions of media were pooled at biweekly intervals over the 3 weeks culture, lyophilized and assayed for tropoelastin using the fastin assay, as previously described [28]. The weight of insoluble elastin, was then compared to that determined by weighing the dry elastin pellet (P2), to affirm low/no loss of elastin material during matrix processing.

2.4.3. *SDS-PAGE and Western Blot analysis for tropoelastin*

SDS-PAGE and Western Blot were performed to selectively and semi-quantitatively confirm the observed biochemical trends with respect to soluble tropoelastin production by cells into the culture media [34]. Pooled aliquots of spent medium collected from atop cell layers after 21 days of culture were lyophilized, assayed for total protein content using a DC protein assay kit (Biorad Corporation, Hercules, CA) as described previously [35]. Sample amounts optimized based on their protein content were then subject to SDS-PAGE and Western Blot. The test cultures subject to Western Blot analyses were selected such as to selectively confirm the previously observed HA fragment size and dose-related trends in tropoelastin synthesis. Briefly, these cell layers were cultured in presence of LMW HA; 0.2 µg/ml (designated as L1), LMW HA; 2 µg/ml (L2), LMW HA; 20 µg/ml (L3), LMW HA; 200 µg/ml (L4), VLMW HA; 2 µg/ml (VL1), VLMW HA; 200 µg/ml (VL2), HMW HA; 2 µg/ml (H1), and HMW HA; 200 µg/ml (H2).

2.4.4. *SDS PAGE/Western Blot*

Optimized sample amounts were mixed with a gel electrophoresis loading buffer (2% (w/v) SDS, 62 mM Tris, 10% (v/v) glycerol, 600 mM dithiothreitol, 30 µg/ml of Bromophenol blue at pH 7.0, the mixture boiled (100 °C, 3 min), then cooled (5 min, 4 °C) and flash-centrifuged (500g, 2 min) to reduce condensation prior to loading onto an electrophoresis gel. Samples were loaded onto 10% (w/v) Polyacrylamide gels (Novex Tris-Glycine gels, Invitrogen Corporation, Carlsbad, CA), with pre-stained protein standards ranging from 10–190 kDa (Benchmark Pre-stained Protein Ladder, Invitrogen) and western blot standards ranging from 20 to 220 kDa (MagicMark XP Western Protein Standards, Invitrogen). Electrophoresis was carried out for 2 h at a constant voltage of 125 V, until the dye front touched the bottom of the gel. Proteins entrapped within the gel were transferred to a prewetted PVDF hydrophobic membrane (Immobilon-P membrane; Millipore Corporation, Billerica, MA; 2 h, 25 V) immersed overnight in blocking buffer (5% (w/v) non-fat

dry milk (Bio-Rad) solubilized in 0.05% (v/v) Tween 20-PBS) and developed using Western Breeze (Chromogenic western blot immunodetection kit, Invitrogen). The primary antibody used for incubation was a polyclonal antibody to elastin (Elastin Products Company, Owensville, MO). Protein bands were visualized and quantified using a Chemi-Imager IS 4400 system (Alpha Innotech, San Leandro, CA). The integrated density value of individual bands corresponds to the amount of tropoelastin in the loaded samples. Thus, the total amount of tropoelastin in the loaded samples was quantified on the basis of a total pixel intensity of 255 that was assigned to totally white and a pixel intensity of zero assigned to completely dark bands. Individual band intensities were then normalized to the corresponding DNA content of the same samples and were finally compared as band intensity on per ng of DNA basis.

2.4.5. *Desmosine assay for detection of cross-linked elastin*

Since desmosine cross-links are unique to stabilized matrix elastin [36], the determination of desmosine levels in the cell-matrix layers is expected to correlate with the amounts of cross-linked elastin and serve as an indirect confirmation of the earlier observed biochemical trends (see Section 2.4.2). Test cell layers subject to the desmosine assay were cultured for 3 weeks with supplements of LMW HA; 0.2 µg/ml (designated as L1), LMW HA; 2 µg/ml (L2), LMW HA; 20 µg/ml (L3), LMW HA; 200 µg/ml (L4), VLMW HA; 2 µg/ml (VL1), VLMW HA; 200 µg/ml (VL2), HMW HA; 2 µg/ml (H1), HMW HA; 200 µg/ml, or no HA supplements (control; ctl). Desmosine content was assayed by an ELISA method [37]. Briefly, cell layers were scraped off, resuspended in 1 ml of 5% (v/v) trichloroacetic acid and centrifuged (3000g, 10 min, 4 °C). The pellet formed was digested with collagenase type VII (Sigma-Aldrich; 12 h, 37 °C) and re-centrifuged (3000g, 10 min, 4 °C) to obtain a supernatant (SI) and a pellet. The pellet was digested with pancreatic porcine elastase type III (Sigma-Aldrich; 12 h, 37 °C) to obtain soluble peptide fractions (SII). Fractions SI and SII were pooled together, hydrolyzed with 6N HCl at 110 °C and dried to powder under nitrogen for 18–24 h. The dried samples were reconstituted in double deionized water and diluted for assay. The wells in micro-titer plates to be used for assay were pre-blocked using desmosine-albumin conjugate (EPC, Owensville, Missouri) in 0.05 M sodium carbonate buffer (pH 9.6, 4 °C), then washed with 0.05% (v/v) Tween-20 and phosphate-buffered saline (PBS) solution (1 h, 25 °C). Desmosine standards/samples were incubated (12 h, 25 °C) with rabbit antiserum to desmosine-hemocyanin conjugate (Elastin Products Company, Owensville, Missouri). After removal of primary antibody solution, the wells were successively incubated with peroxidase-conjugated anti-rabbit IgG 0.05% (v/v) Tween 20-PBS solution (2 h, 25 °C). Finally, the colorimetric compound 2,2'-Azino-bis (3-ethylbenzothiazoline-6-sulfonic acid), (Sigma) 0.08 mg in 0.1 M citrate phosphate buffer containing 0.003% (v/v) hydrogen peroxide, (pH 4), was added to the wells and incubated (1 h, 25 °C). Absorbances were read in a UV-spectrophotometer at $\lambda = 405$ nm.

2.5. *Light microscopy*

Light microscopy was used to determine HA fragment- or dose-specific changes to cell phenotype, if any. The cell layers were cultured in the presence of HMW HA (200 µg/ml), LMW HA (200 µg/ml), VLMW HA (200 µg/ml) and no HA (controls), and were periodically imaged on an Axiovert 200 (Carl Zeiss, Thornwood, NY).

2.6. *Immunofluorescence detection of elastin and collagen*

Immunofluorescence was used to confirm the presence of elastin and collagen in select test cell layers, cultured in the presence of HMW HA (200 µg/ml), LMW HA (200 µg/ml), VLMW HA (200 µg/ml) and no HA (controls), respectively. Briefly, the cell layers were rinsed with 1% (v/v) PBS at 37 °C, fixed with 4% (v/v) paraformaldehyde for 10 min, rinsed again in an excess of cold PBS, and labeled with Alexa 488 Phalloidin, a fluorescent probe for smooth muscle cell actin (1:20 dilution; 20 min,

25 °C). Cell layers were then treated with a blocking buffer containing 5% (v/v) donkey serum, and 0.3% (v/v) Triton-X detergent in 1(X) PBS, in order to reduce non-specific binding of the secondary antibody. Cell layers were incubated (1 h, 37 °C), rinsed and treated with a Cy5-conjugated donkey anti-rabbit IgG secondary antibody (1:500 dilution; 1 h, 25 °C). Cell nuclei were labeled with the nuclear stain 4', 6-diamino-2-phenylindole dihydrochloride (DAPI; Molecular Probes) dissolved in PBS. Labeled cell layers were mounted with Vectashield (Vector Laboratories, Burlingame, CA). Adult rat aortal elastin served as a positive control for immunolabeling. Prior to labeling, cell layers were quenched in ethanol/phosphomolybdic acid mixture for 15 min to block the collagen autofluorescence. Negative control specimens (both cell layer- and tissue-sections) were not treated with the primary antibody against elastin or collagen.

2.7. Matrix ultrastructure

TEM was used to selectively compare the distribution and ultrastructure of matrix elastin between cell layers cultured with or without exogenous bolus of HA. For TEM, the adhered cell layers were fixed in 2.5% (v/v) glutaraldehyde, post-fixed in 1% (v/v) OsO₄, dehydrated with ethanol, then embedded in resin, cut into 70 nm thick sections and finally stained with uranyl acetate and lead citrate. Test cell layers received HMW HA (200 and 0.2 μg/ml), and VLMW HA (200 and 0.2 μg/ml). Control cell layers received no HA.

2.8. Fibrillin-mediated organization of matrix elastin

Immunogold labeling and TEM were used to detect presence of fibrillin, a scaffolding protein that normally precedes the deposition of elastin in the ECM [38]. 21 day-old cell layers that received HMW HA (200 μg/ml) supplements, were incubated with a rabbit anti-rat primary fibrillin-I antibody (20% (v/v); 14 h, dark; (EPC)), then rinsed and treated with a goat anti-rabbit IgG conjugated with gold nanoparticles (10 nm; Structure Probe, Inc., West Chester, PA) diluted 1:3 (v/v) in 20 mM TRIS-HCl, pH 8.2 in PBS with 0.1% (v/v) BSA. The labeled specimens were then processed as described in Section 2.7, stained with 2% (v/v) uranyl acetate, and finally resin embedded and sectioned. Cell layers untreated with the primary antibody served as negative controls.

2.9. Statistical analysis

All experiments were performed in triplicate, unless otherwise mentioned. Statistical significance between and within groups was determined using Microsoft Excel's statistical function for *t*-tests, assuming unequal variance and two-tailed distribution. Differences were considered statistically significant at $p < 0.05$. Quantitative results are reported as mean \pm standard deviation.

3. Results

3.1. Cell proliferation

Control cell layers proliferated to 1.6 ± 1.6 times the original seeded cell number at 21 days of culture (Fig. 1). HA-supplemented cultures showed similar (HMW HA) or higher (LMW, VLMW HA) levels of proliferation that inversely correlated to HA fragment size (Fig. 1), although there was no significant correlation between proliferation ratios and added HA dose within each size group.

3.2. Biochemical quantification of extracellular matrix

3.2.1. Soluble tropoelastin synthesis

The measured tropoelastin amounts were normalized to the average DNA content. In general, cell layers supplemented with HMW HA showed levels of tropoelastin output that were comparable to that produced in control cell layers ($P \geq 0.05$). Although slight inhibition of elastin synthesis was observed at low doses, a significant stimulation in elastin synthesis was observed at higher doses (Fig. 2(a)). Smaller HA fragments significantly inhibited tropoelastin synthesis in inverse correlation to fragment size for LMW and VLMW HA ($p < 0.001$ for both LMW vs. and VLMW vs. control). No dose-related effects on tropoelastin synthesis were noted

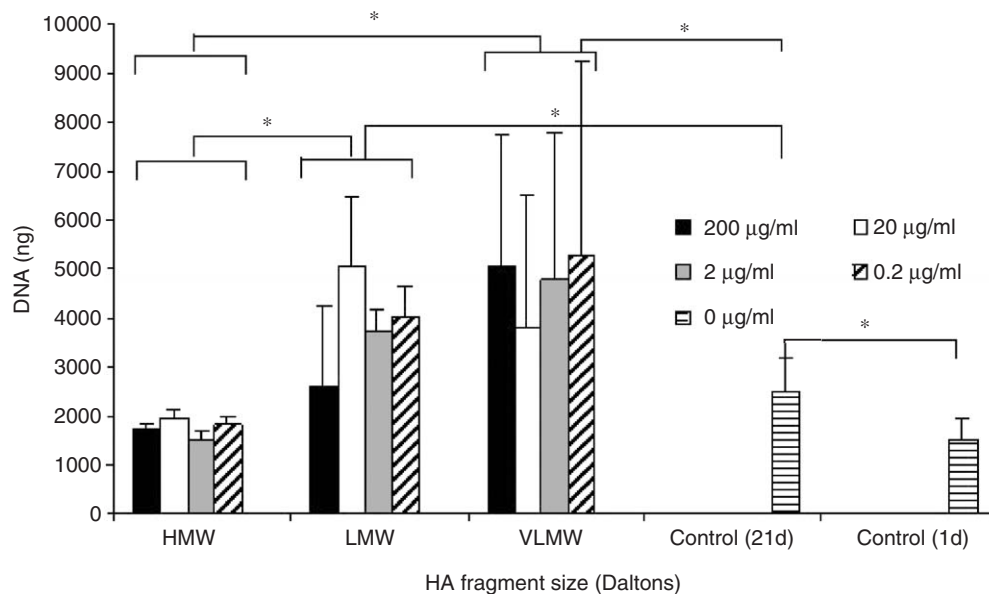


Fig. 1. Effect of exogenous HA supplements on proliferation of cultured SMCs. Shown are the mean \pm SD of DNA content of cell layers cultured in the presence of HMW, LMW and VLMW-HA (200, 20, 2 and 0.2 μg/ml) or in their absence (controls) ($n = 3$). All cells were seeded identically and harvested for analysis at 21 days. Inter-fragment size differences were deemed significant for $p < 0.05$ (*).

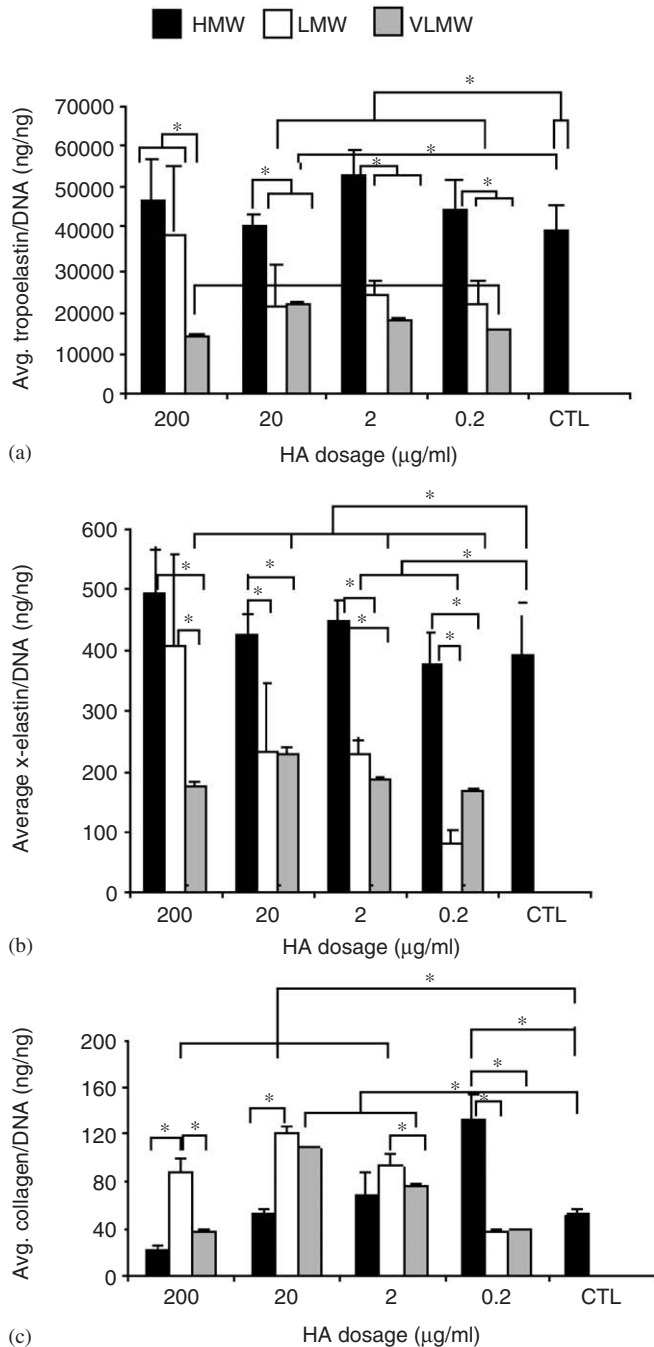


Fig. 2. Effects of exogenous HA on matrix synthesis by adult SMCs. Shown are the mean \pm SD of average tropoelastin (a), matrix elastin (b) and collagen (c) amounts synthesized within HA-supplemented and non-HA control cell layers. Values are shown normalized to cellular DNA content at 21 days of culture ($n = 3$ /case). Significance of differences in elastin/collagen synthesis were deemed for $p < 0.05$ and are indicated by *.

except at high doses (200 µg/ml) of LMW HA, when tropoelastin output approached that produced by cell layers exposed to that of HMW HA or controls ($p = 0.56$ HMW vs. LMW at dose of 200 µg/ml).

3.2.2. Synthesis of cross-linked matrix elastin

Elastin incorporated into the extracellular matrix was measured as a sum of two fractions, namely, a highly cross-

linked, alkali-insoluble elastin pellet, and a cross-linked alkali-soluble fraction. In general, the total DNA-normalized output of matrix elastin mirrored the HA fragment size-specific trends reported for tropoelastin (see Section 3.2.1). HMW HA suppressed elastin matrix synthesis at very low doses (0.2 µg/ml), induced a stimulatory effect at intermediate doses (2 µg/ml), which increasingly waned at higher doses (Fig. 2(b)). However, in all cases, the differences vs. controls were not significant ($p = 0.4$). In comparison, fragmented HA inhibited elastin matrix synthesis to an extent that inversely correlated to HA fragment size ($p < 0.03$ for 200 vs. 2 mg/ml and 0.2 mg/ml for LMW HA). As noted with synthesis of tropoelastin, VLMW HA did not have a dose-specific effect on matrix elastin synthesis, although at high doses (200 µg/ml), LMW HA induced significantly higher levels of elastin synthesis, closely approaching production levels as seen in control cultures.

3.2.3. Collagen synthesis

Exogenous HA had a dose-dependant effect on collagen synthesis (Fig. 2(c)). Within each HA fragment-size group, peak induction of collagen synthesis occurred at specific doses that inversely correlated to HA fragment size. Thus, peak cellular collagen synthesis for HMW, LMW, and VLMW HA occurred at doses of 0.2, 20 and 20 µg/ml, respectively. Also, the magnitude of these peak-collagen amounts positively correlated to size of HA fragments.

3.2.4. Western blot/SDS PAGE for tropoelastin

Cell cultures supplemented with HMW HA synthesized the same levels of tropoelastin as did control cultures, while those cultured in presence of lower-sized HA fragments inhibited elastin synthesis relative to controls in inverse correlation to fragment size (Fig. 3).

3.2.5. Desmosine assay for cross-linked matrix elastin

Desmosine amounts measured in cell layers cultured with HMW HA were similar to that produced in control cultures. Desmosine content was severely inhibited relative to controls in cell layers supplemented with LMW or VLMW HA (Fig. 4).

3.3. Cell morphology

No visible changes to cell morphology were observed between HA-supplemented cell cultures and control cell cultures at early or late culture times, although beyond 2 weeks of culture cell clumps were seen in the former, but not the latter cultures. The number and size of these cell clumps did not show any correlation to HA fragment size or dose.

3.4. Immunodetection of elastin and collagen

The matrix of 21 day-old cell layers was found to contain elastin as a significant component. Test cell layers showed

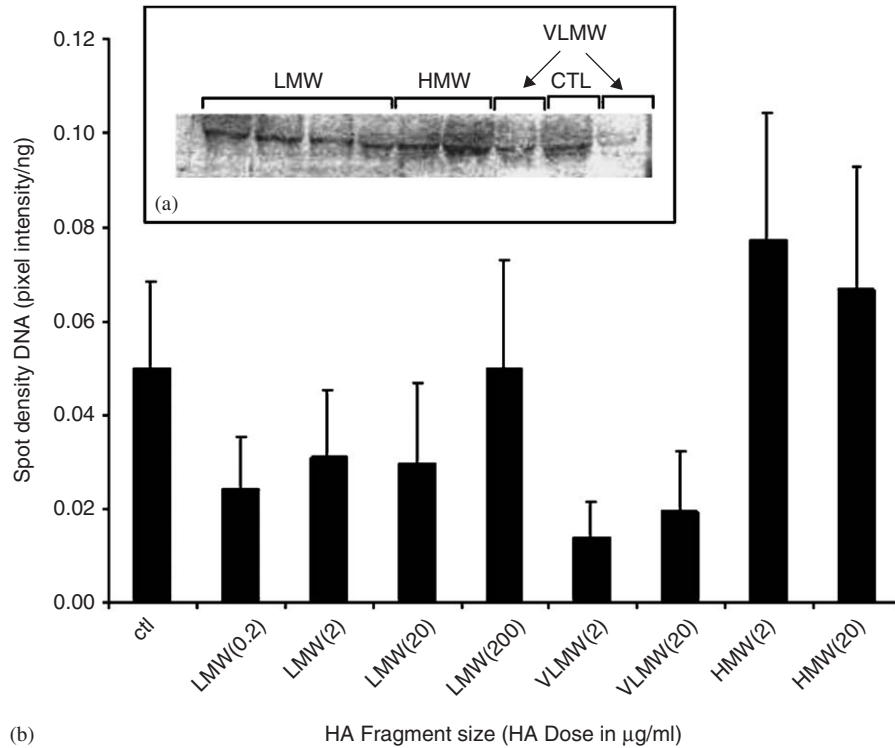


Fig. 3. Confirmation of tropoelastin production trends by SDS-PAGE/Western blot. Panel (a) shows a sample blot containing bands corresponding to tropoelastin produced in the presence of HA of designated fragment sizes or its absence (controls). Panel (b) shows the mean \pm SD of average spot densities (pixel intensities) of shown bands normalized to the DNA content of the corresponding HA supplemented or control cell layers ($n = 3/\text{size/dose}$). The trends agree with tropoelastin production, measured biochemically and shown in Fig. 2(a).

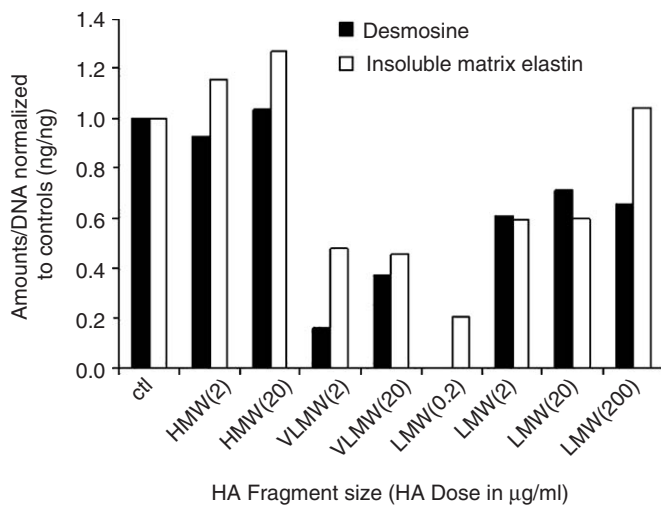


Fig. 4. Comparison of the size- and dose-specific effects of exogenous HA supplements on desmosine and matrix elastin content of SMC cultures. Shown are mean measured amounts of desmosine/DNA (ng/ng) and matrix elastin/DNA (ng/ng) normalized to corresponding measurements in control cell layers (no HA), plotted as functions of HA fragment size and dose ($n = 3/\text{case}$).

numerous DAPI-stained nuclei (blue) engulfed in a mass of homogenous elastin or collagen matrix (red; Figs. 5(a and b)); the elastin was not organized into lamellae as in aortic tissue (Fig. 5(e)) and collagen was sparse and localized in distribution, unlike aortic tissue where collagen is plentiful

(Fig. 5(f)). Cell layers and aortae not treated with the primary antibody to rat elastin and collagen (negative controls) confirmed the absence of non-specific binding of the Cy-5 fluorophore (Figs. 5(c and d)).

3.5. Ultra-structure of elastin and collagen in the matrix

Cell layers cultured in the presence and absence of HA both contained multiple stacked layers of cells at 21 days (Fig. 6(a–d)). The density of elastin deposits within the cell layers mirrored the HA size- and dose-specific trends established through biochemical analyses ($n = 30/\text{micrographs/case}$); the density of elastin within control cell layers and those supplemented with HMW HA (200 $\mu\text{g/ml}$) appeared similar, while appearing much more dense compared to within cell layers cultured in presence of VLMW HA (200 $\mu\text{g/ml}$). Again, the relative similarity in the density of elastin deposits between cell layers that received 200 $\mu\text{g/ml}$ of HMW HA and those that received 0.2 $\mu\text{g/ml}$ of HMW HA semi-quantitatively confirmed the lack of a dose effect within this tested group. In most cases, the cell layers exhibited relatively poor native tissue-like organization into fibers and fiber bundles; rather the cell layers contained amorphous elastin clumps, many of which exhibited cross-sectional diameters similar to that of elastin fibers, although only few fibers were seen in axial orientation. The exceptions were cell layers that received low doses (0.2 $\mu\text{g/ml}$) of HMW which exhibited several

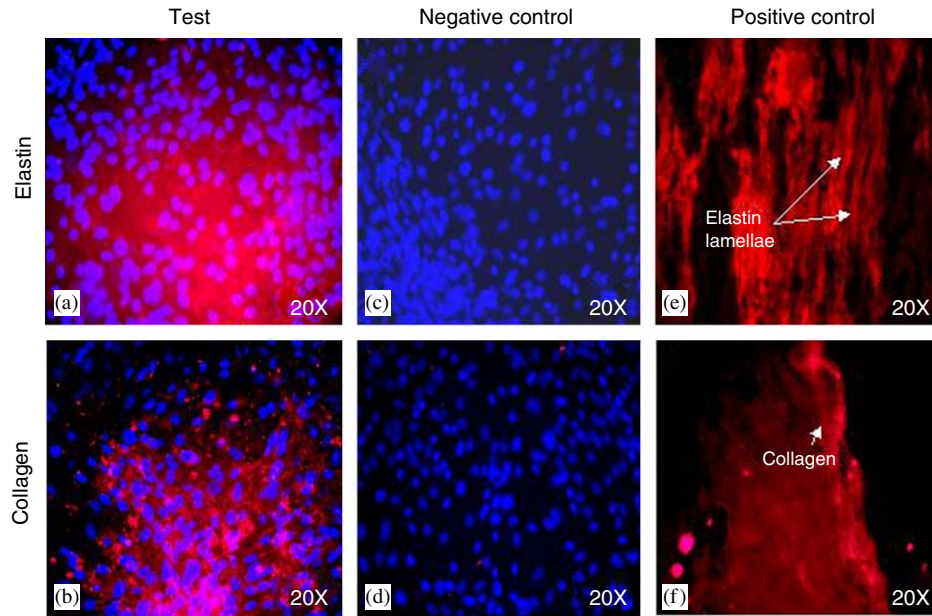


Fig. 5. Immunodetection of elastin and collagen within SMC layers. (a) and (b) show presence of elastin and collagen respectively (red) following 21 days of culture in the presence of HMW HA (200 $\mu\text{g}/\text{ml}$). Coloration due to elastin or collagen is absent in cell layers not treated with the respective primary antibodies (negative controls; c, d). The specificity of the primary antibodies used to detect rat elastin and collagen was confirmed by localization of red fluorescence along the elastic lamellae and adventitia of rat aortae (positive controls; e, f). Nuclei were stained with DAPI (blue).

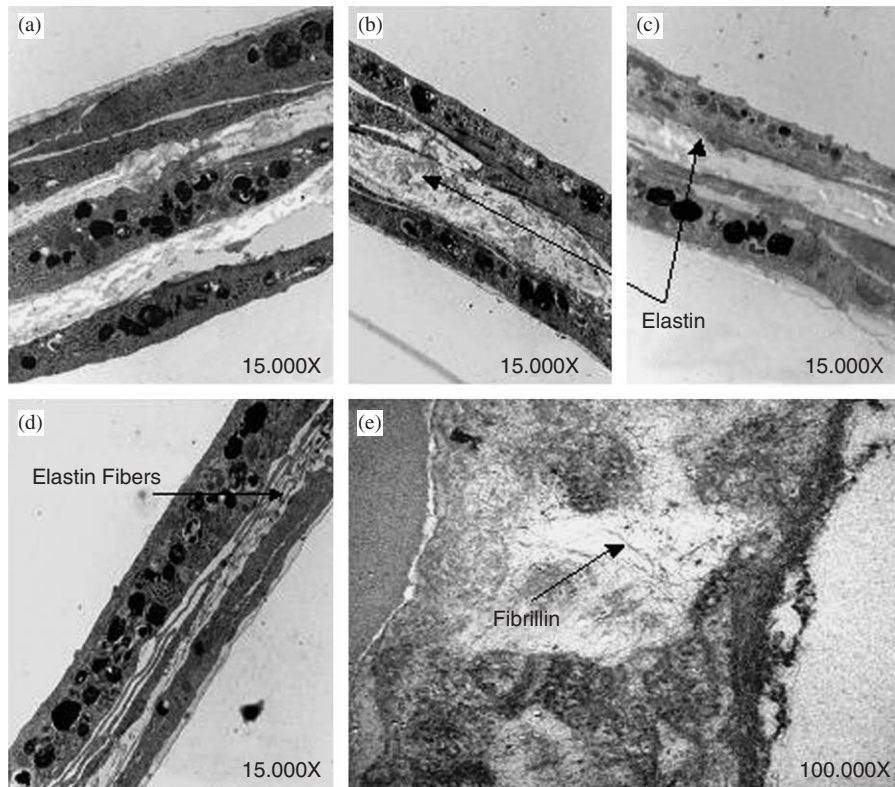


Fig. 6. Matrix ultrastructure and fibrillin-mediated elastin deposition. Shown are representative transmission electron micrographs of 21 day-old cell layers cultured in the presence of HMW HA (200 $\mu\text{g}/\text{ml}$; b), VLMW HA (200 $\mu\text{g}/\text{ml}$; c) or HMW HA (0.2 $\mu\text{g}/\text{ml}$; d) or in its absence (a). In each case, representative images were selected from nearly 20 captured micrographs. A qualitative comparison of the amounts of elastin deposited within these cell layers suggests no HA dose effects (compare b, d, and a, b), but shows HA fragment size effects (compare b and c). A mesh of fibrillin microtubules surrounded the indicated amorphous elastin clumps (e).

longitudinally extended elastin clumps, closely resembling fibers when viewed at high magnifications ($60,000\times$).

3.6. Microfibrillar basis for elastin deposition

Both control and test cell layers tested positive for fibrillin, which appeared as darkly stained microfibrillar networks at the periphery of amorphous elastin clumps (Fig. 6(e)). Such fibrils were not visible in non-immunogold-labeled cell layers. The average fibrillin strand length was 57 ± 7 nm.

4. Discussion

The long-term objective of our current research is to develop scaffolds based on GAGs, specifically HA, to regenerate structurally and functionally faithful vascular elastin matrices on demand. Such matrices are expected to reinstate the crucial structural configurations and cell signaling pathways, regulated by elastin, within blood and cell signaling vessels, which are lost when elastin is congenitally absent, malformed, or degraded due to disease or injury.

The choice of HA scaffolds for elastic regeneration is based on previous observations that implicates several GAG types (HA, heparin sulfate) directly or indirectly in vivo mechanisms of elastin synthesis, maturation and organization. Also, in various tissue types [24–26,37–40] fragmented HA and HA oligosaccharides have been shown to be more biologically active than long-chain HA, and are likely responsible for eliciting elastogenic responses from cells, although long-chain HA may play a role in facilitating matrix deposition. Since HA fragments can also potentially elicit inflammatory cell responses, the design of elastogenic scaffolds based on a mixture of HA and its fragments must follow a thorough investigation into the size-specific effects of HA on desired (e.g., elastogenic), and undesired (e.g., inflammatory) cell responses. The first aspect, namely elastogenic responses, is investigated in the current study.

An exogenous supplementation model is a simple and frequently adopted method to assess dose-specific responses to growth factors/signaling molecules, and has been extensively used to study cell (e.g., chondrocytes, fibroblasts) responses to HA [41,42]. Since biomechanical stimuli proffered by cell–scaffold contact and continuous long-term HA–cell receptor interaction likely play important roles in modulating cell responses, an exogenous supplementation model may not completely replicate cell responses to an HA scaffold. However, such a model can provide vital clues to understanding the size- and dose-specific elastogenic responses of SMCs to HA and also cell responses to biodegradation-generated HA fragments when vascular implants based on HA are deployed in vivo.

We saw that HMW and LMW, VLMW-HA induced marginal inhibition, and enhancement of cell proliferation, respectively, relative to control cell cultures. This finding

complies with results from other studies where shorter HA fragments have been reported with other cell types such as chondrocytes [41], endothelial cells [30] and fibroblasts [42] to be pro-cell-proliferative and angiogenic unlike native HMW HA. Also, the observed results are in agreement with our earlier published observations of greatly enhanced cell proliferation atop cross-linked gels containing a mixture of long-chain HA and smaller fragments, relative to one containing long-chain HA alone [28]. Although a detailed investigation into the mechanisms underlying these results is beyond the scope of this study, a possible explanation may lie in the ability of non-long-chain native HA fragments to cause phosphorylation of the cell-surface glycoprotein HA receptor, CD44, which extracellularly interacts with HA intracellularly with the cell cytoskeleton [43]. Possibly, smaller HA fragments, but not long-chain HA, phosphorylates CD44, and further activate a cytoplasmic cascade of events ultimately inducing cell proliferation, as described previously [43]. Alternatively, low cell density and high initial levels of cell proliferation rates (>1 day) may correlate with increased endogenous HA synthesis and accumulation that inhibit cell proliferation through a feedback mechanism [44]. Possibly, the high negatively charged long-chain HA may somehow inhibit cell proliferation, although this alone may not be a determinant of the observed effects because other more negatively charged GAGs (e.g. dextran sulfate) do not particularly inhibit cell proliferation [45]. Unlike results reported with other cell types, which demonstrated the proliferation-inhibitory effects of high concentrations (1000 $\mu\text{g/ml}$) of HMW HA and proliferation-stimulation effects of fragmented HA at low concentrations, we did not observe any dose effects. These differences may be due to the respective selections of tested HA sizes and doses (>1000 vs. 200 $\mu\text{g/ml}$ in this study). While the maximal HA doses adopted in this study roughly correspond to the typical HA concentration within earlier tested cross-linked HA gels (hylans) [28], further extrapolation of the dose range may indicate dose-specific effects on cell proliferation. HMW-HA stimulated elastin production beyond that in control cultures, at high doses (200 $\mu\text{g/ml}$), but increasingly inhibited the same at lower doses. This dose effect was much more pronounced for synthesis of matrix elastin than for soluble tropoelastin. A comparison of the trends pertaining dose-specific effects of HMW-HA on cell proliferation and elastin synthesis, suggests that the latter is likely regulated via a different mechanism, possibly preferred post-translational coacervation and cross-linking of soluble tropoelastin at the highly negatively charged HA surface. Likely, such coacervation is a function of cumulative negative charge of the HA molecule, which is in turn determined by fragment size. The same reasons can be evoked to explain a similar trend observed when cell cultures are supplemented instead with LMW-HA.

An unexpected finding was that LMW and VLMW HA both inhibited tropo- and matrix elastin synthesis relative to controls, and to extents that correlated inversely to

fragment size. Previous studies showed more exuberant elastin synthesis by cells cultured atop gels containing HMW and fragmented HA, than those cultured on gels containing HMW HA alone [28].

It was earlier hypothesized that long-chain HA was bioinert and only useful from the perspective of producing gels that were biocompatible and possessed some mechanical integrity; smaller-sized fragments were the ones that elicited enhanced cell adherence, proliferation and matrix synthesis. Suggestably, while HA fragments may elicit enhanced proliferative responses among SMCs, the slight enhancement in matrix elastin synthesis, may be purely due to the greater efficiency of LOX-mediated cross-linking when soluble tropoelastin preferentially coacervates at the negatively charged HA surfaces [26]. However, the lack of any HA-mediated enhancement in per cell elastin output as previously determined for cells cultured on HA gels suggests vital differences in cell response to HA, when delivered exogenously and or as a substrate. Previous studies have implicated HA and other GAGs in stabilizing elastin fibers against elastase degradation [27]. In the current study, elastase activity was not blocked over the 21 days of culture. Thus, it is likely that the observed differences in elastin output are due to the combined influence of two possible factors namely, HA-mediated stabilization of elastin, and HA-induced differences in cellular elastin output. The relative influence of these factors will be investigated in a future study.

The differences in desmosine cross-link content of selected test and control cell layers mirrored that in their respective differences in insoluble matrix elastin content, confirming the observed biochemical trends. Since each of these assays was performed on replicate and not the same cell layers, the amounts of desmosine cross-links may not be normalized to the respective elastin amounts. Thus, it is yet uncertain if HA influence on cross-link density is size- or dose-specific.

Collagen synthesis was determined to be a function of both added HA-chain length and dose. Generally, both VLMW and LMW HA stimulated cellular collagen output in direct correlation to added dose, with peak output attained at $>20\ \mu\text{g}/\text{ml}$, and relative inhibition observed at higher HA doses. A likely explanation for the observed dose-specificity within each MW group is increasing levels of CD44-HA interaction, which signal cells to upregulate collagen production until saturation is attained. Further, added HA likely down-regulates CD44 receptor expression inhibiting collagen synthesis via a negative feedback mechanism. A comparison of peak collagen amounts synthesized by cells cultured with HMW HA and shorter HA fragments, suggests that impact of CD44-HA interactions are additive as more HA monomers are added.

Most elastin in test and control (no HA) cell layers was deposited in the form of amorphous clumps. Within this group, many clumps appeared circular and measured roughly 100 nm across, supporting our assumption that these are transverse-sections of elastin fibers, several of

which were seen in axial orientation. The presence of fibrillin microtubule networks surrounding elastin clumps, essential precursors to elastin fiber organization, suggests that elastic fiber organization in presence of HA proceeds via normal fibrillin-mediated mechanisms. The predominance of amorphous elastin clumps over elastin fibers may be an outcome of the failure to concomitantly provide essential biomechanical, or biochemical stimuli in the form of growth factors (e.g., TGF- β), which have been suggested previously to increase cross-linking and induce elastic fiber organization [46]. The greater density of elastin fibers in cell layers cultured with HMW HA than smaller HA fragments, implicates HMW HA in the post-translational maturation of matrix elastin, although this must be rigorously confirmed. The complete absence of lamellar elastin unlike that produced by cells cultured atop hylan gels [28], may be due to the lack of HA derivatization or chemical cross-linking, which may influence elastin deposition as a lamellar layer. Again, the impact of actual long-term HA-cell contact in elastin organization cannot be discounted.

Although the effects of HA oligos (e.g., hexamers) have not been yet assessed, it is already apparent that the exogenous supplementation model does not necessarily emulate cell culture on hylan gels particularly with regard to generation of lamellar elastin [28]. Thus, clearly, an exogenous HA supplementation model is inadequate in predicting cell response to HA culture substrates. The true effects of HA size or dose on cell response may likely be better predicted by long-term cell contact with surface-tethered HA/HA fragments.

5. Conclusions

In summary, the current work has evaluated the efficacy of a much adopted HA exogenous supplementation model in predicting elastogenic SMC responses to HA scaffold composition investigated in a previous study. The results of the current study highlight vital differences in elastogenic cell responses to either of the two HA delivery methods, likely due to absence of prolonged HA/HA fragment-cell receptor (CD44) contact and biomechanical substrate-derived stimuli. Notably, these differences pertain to both the quantity as well as qualitative ultrastructural organization of elastin within the cell layer, with the notable absence of the lamellar elastic layer, produced atop HA scaffolds. Despite this, the current work conclusively demonstrates that elastogenic cell responses to HA, functions of HA fragment size and dose. Ongoing work will investigate the size and dose-specific effects of surface-tethered HA on elastin synthesis and organization, which will likely better explain the observed cell response to HA gels. The current results are nevertheless important towards designing composition-optimized HA scaffolds for regenerating vascular elastin structures.

Acknowledgements

This study was funded by the American Heart Association (SDG 0335085N), the National Science Foundation (0132573) and National Institutes of Health (CO6 RR018823). The authors would also like to acknowledge Dr. Sumita Bandopadhyay, Department of Biochemistry at MUSC for her help with performing SDS-PAGE/Western Blot.

References

- [1] Ross R, Bornstein P. Elastin fibers in the body. *Sci Am* 1971;224(6):44–52.
- [2] Parks WC, Pierce RA, Lee KA, Mecham RP. The extracellular matrix. *Adv Mol Cell Biol* 1993;6:133–82.
- [3] Wolinski H, Glasgow SA. Lamellar unit of aortic medial structure and function. *Circ Res* 1967;20:90–111.
- [4] Raines EW. The extracellular matrix can regulate vascular cell migration, proliferation, and survival: relationships to vascular disease. *Int J Exp Pathol* 2000;81(3):173–82.
- [5] Spofford CM, Chilian WM. Mechanotransduction via the elastin-laminin receptor (ELR) in resistance arteries. *J Biomech* 2003;36(5):645–52.
- [6] Li DY, Brooke B, Davis EC, Mecham RP, Sorensen LK, Boak BB, et al. Elastin is an essential determinant of arterial morphogenesis. *Nature* 1998;93(6682):276–80.
- [7] Karnik SK, Brooke BS, Bayes-Genis A, Sorensen L, Wythe JD, Schwartz RS, et al. A critical role for elastin signaling in vascular morphogenesis and disease. *Development* 2003;130(2):411–23.
- [8] Brooke BS, Bayes-Genis A, Li DY. New insights into elastin and vascular disease. *Trends Cardiovasc Med* 2003;13(5):176–81.
- [9] Sandberg LB, Soskel NT, Leslie JG. Elastin structure, biosynthesis, and relation to disease states. *N Engl J Med* 1981;304(10):566–79.
- [10] Stock UA, Sakamoto T, Hatsuoka S, Martin DP, Nagashima M, Moran AM, et al. Patch augmentation of the pulmonary artery with bioabsorbable polymers and autologous cell seeding. *J Thorac Cardiovasc Surg* 2000;120(6):1158–67.
- [11] Kim BS, Nikolovski J, Bonadio J, Smiley E, Mooney DJ. Engineered smooth muscle tissues: regulating cell phenotype with the scaffold. *Exp Cell Res* 1999;251(2):318–28.
- [12] Berglund JD, Nerem RM, Sambanis A. Incorporation of intact elastin scaffolds in tissue-engineered collagen-based vascular grafts. *Tissue Eng* 2004;10(9–10):1526–35.
- [13] Johnson DJ, Robson P, Hew Y, Keeley FW. Decreased elastin synthesis in normal development and in long-term aortic organ and cell cultures is related to rapid and selective destabilization of mRNA for elastin. *Circ Res* 1995(6):1107–13.
- [14] Hoffman AS. Hydrogels for biomedical applications. *Ann NY Acad Sci* 2001;944:62–73.
- [15] Sodian R, Sperling JS, Martin DP, Egozy A, Stock U, Mayer Jr JE, et al. Fabrication of a trileaflet heart valve scaffold from a polyhydroxyalkanoate biopolymer for use in tissue engineering. *Tissue Eng* 2000;6(2):183–8.
- [16] Allaire E, Guettier C, Bruneval P, Plissonnier D, Michel JB. Cell-free arterial grafts: morphologic characteristics of aortic isografts, allografts, and xenografts in rats. *J Vasc Surg* 1994;19(3):446–56.
- [17] Guidoin R, Noel HP, Dube S, de Estable-Puig RF, Marois M, King M. The fate of human umbilical vein grafts as an infrarenal aortic substitute in monkeys. *J Vasc Surg* 1985;2(5):715–23.
- [18] Courtman DW, Pereira CA, Kashef V, McComb D, Lee JM, Wilson GJ. Development of a pericardial acellular matrix biomaterial: biochemical and mechanical effects of cell extraction. *J Biomed Mater Res* 1994;28(6):655–66.
- [19] Bailey MT, Pillarisetti S, Xiao H, Vyavahare NR. Role of elastin in pathologic calcification of xenograft heart valves. *J Biomed Mater Res A* 2003;66(1):93–102.
- [20] Urry DW, Pattanaik A, Xu J, Woods TC, McPherson DT, Parker TM. Elastic protein-based polymers in soft tissue augmentation and generation. *J Biomater Sci Polym Ed* 1998;9(10):1015–48.
- [21] Wright ER, Conticello VP. Self-assembly of block copolymers derived from elastin-mimetic polypeptide sequences. *Adv Drug Deliv Rev* 2002;54(8):1057–73.
- [22] Lee SH, Kim BS, Kim SH, Choi SW, Jeong SI, Kwon IK, et al. Elastic biodegradable Poly (glycolide-co-caprolactone) scaffold for tissue engineering. *J Biomed Mater Res A* 2003;66(1):29–37.
- [23] Opas M. Substratum mechanics and cell differentiation. *Int Rev Cytol* 1994;150:119–37.
- [24] Wight TN. Versican: a versatile extracellular matrix proteoglycan in cell biology. *Curr Opin Cell Biol* 2002;14(5):617–23.
- [25] Fornieri C, Baccarani-Contri M, Quaglino Jr D, Pasquali-Ronchetti I. Lysyl oxidase activity and elastin/glycosaminoglycan interactions in growing chick and rat aortas. *J Cell Biol* 1987;105(3):1463–9.
- [26] Bressan GM, Pasquali-Ronchetti I, Fornieri C, Mattioli F, Castellani I, Volpin D. Relevance of aggregation properties of tropoelastin to the assembly and structure of elastic fibers. *J Ultrastruct Mol Struct Res* 1986;94(3):209–16.
- [27] Cantor JO, Turino GM. Can exogenously administered hyaluronan improve respiratory function in patients with pulmonary emphysema? *Chest* 2004;125(1):288–92.
- [28] Ramamurthi A, Vesely I. Evaluation of the matrix-synthesis potential of crosslinked hyaluronan gels for tissue engineering of aortic heart valves. *Biomaterials* 2005;26(9):999–1010.
- [29] Masters KS, Shah DN, Leinwand LA, Anseth KS. Crosslinked hyaluronan scaffolds as a biologically active carrier for valvular interstitial cells. *Biomaterials* 2005;26(15):2517–25.
- [30] Takahashi Y, Li L, Kamiryo M, Asteriou T, Moustakas A, Yamashita H, et al. Hyaluronan fragments induce endothelial cell differentiation in a CD44- and CXCL1/GRO1-dependent manner. *J Biol Chem* 2005;280(25):24195–204.
- [31] Noble PW. Hyaluronan and its catabolic products in tissue injury and repair. *Matrix Biol* 2002;21(1):25–9.
- [32] Labarca C, Paigen K. A simple, rapid, and sensitive DNA assay procedure. *Anal Biochem* 1980;102:344–52.
- [33] Liao J, Vesely I. Relationship between collagen fibrils, glycosaminoglycans, and stress relaxation in mitral valve chordae tendineae. *Ann Biomed Eng* 2004;32(7):977–83.
- [34] Stegeman H, Stalder K. Determination of hydroxyproline. *Clin Chim Acta* 1967;18:267–73.
- [35] Baranska-Rybak W, Sonesson A, Nowicki R, Schmidtchen A. Glycosaminoglycans inhibit the antibacterial activity of LL-37 in biological fluids. *J Antimicrob Chemother* 2005, [<http://jac.oxfordjournals.org/cgi/reprint/dki460v1>].
- [36] Cantor JO, Shteyngart B. How a test for elastic fiber breakdown products in sputum could speed development of a treatment for pulmonary emphysema. *Med Sci Monit* 2004;10(1):RA1–4.
- [37] Viglio S, Iadarola P, Lupi A, Trisolini R, Tinelli C, Balbi B, et al. MEKc of desmosine and isodesmosine in urine of chronic destructive lung disease patients. *Eur Respir J* 2000;15(6):1039–45.
- [38] Rock MJ, Cain SA, Freeman LJ, Morgan A, Mellody K, Marson A, et al. Molecular basis of elastic fiber formation. Critical interactions and a tropoelastin-fibrillin-1 cross-link. *J Biol Chem* 2004;279(22):23748–58.
- [39] Buczek-Thomas JA, Chu CL, Rich CB, Stone PJ, Foster JA, Nugent MA. Heparan sulfate depletion within pulmonary fibroblasts: implications for elastogenesis and repair. *J Cell Physiol* 2002;192(3):294–303.
- [40] Baccarani-Contri M, Vincenzi D, Cicchetti F, Mori G. Immunocytochemical localization of proteoglycans within normal elastin fibres. *Eur. J. Cell Biol.* 1990;53:305–12.
- [41] Akmal M, Singh A, Anand A, Kesani A, Aslam N, Goodship A, et al. The effects of hyaluronic acid on articular chondrocytes. *J Bone Joint Surg Br* 2005;87(8):1143–9.

- [42] Croce MA, Boraldi F, Quaglino D, Tiozzo R, Pasquali-Ronchetti I. Hyaluronan uptake by adult human skin fibroblasts in vitro. *Eur J Histochem* 2003;47(1):63–73.
- [43] Slevin M, Krupinski J, Kumar S, Gaffney J. Angiogenic oligosaccharides of hyaluronan induce protein tyrosine kinase activity in endothelial cells and activate a cytoplasmic signal transduction pathway resulting in proliferation. *Lab Invest* 1998;78(8):987–1003.
- [44] Turley EA, Noble PW, Bourguignon LY. Signaling properties of hyaluronan receptors. *J Biol Chem* 2002;277(7):4589–92.
- [45] Goldberg RL, Toole BP. Hyaluronate inhibition of cell proliferation. *Arthritis Rheum* 1987;30(7):769–78.
- [46] Shanley CJ, Gharaee-Kermani M, Sarkar R, Welling TH, Kriegel A, Ford JW, et al. Transforming growth factor-beta 1 increases lysyl oxidase enzyme activity and mRNA in rat aortic smooth muscle cells. *J Vasc Surg* 1997;25(3):446–52.